Picosecond Dynamics of Simple Monosaccharides As Probed by NMR and Molecular Dynamics Simulations

Philip J. Hajduk, David A. Horita, and Laura E. Lerner*

Contribution from the Department of Chemistry, University of Wisconsin, 1101 University Avenue, Madison, Wisconsin 53706

Received April 6, 1993®

Abstract: Carbon-13 T_1 and NOE measurements have been performed on D-glucose, D-galactose, D-mannose, and L-idose, and molecular dynamics calculations have been performed on α-D-glucose and α-L-idose. Order parameters were obtained both from the relaxation data, at various field strengths and temperatures, and from the dynamics simulations. Results from both calculations and experimental data indicate that, on the picosecond time scale, all carbon sites in the sugar ring have some degree of motional freedom, most likely in the form of ring librations, but that both the ring and hydroxymethyl carbons maintain a single global conformation. The rate of interconversion among hydroxymethyl rotamers for all sugars and the various ring conformations for idose would have to occur on a time scale of 10^{-9} to 10^{-3} s to account for the experimental data. The results presented here have implications for the flexibility of idose-related residues in heparin and heparan sulfate, and for the relationship between restricted rotation of hydroxymethyl groups and intramolecular hydrogen bonds.

Introduction

There has been considerable interest in the conformational flexibility and dynamics of carbohydrates in aqueous solution. For example, idose and many of its derivatives have been investigated on the basis of ^1H–^1H spin coupling constants and molecular mechanics and dynamics studies and have been shown to exist in several ring conformations.[1-6] Casu and co-workers have suggested that this flexibility is related to specific interactions of heparin and heparan sulfate with proteins such as antithrombin III.[7] In contrast, several authors have proposed that sucrose is unusually rigid.[8,9] This rigidity is attributed to hydrogen bonds between the pyranose and furanose moieties which have been claimed to persist even in solution.[9] However, recent evidence from NMR of the sucrose hydroxyl protons suggests these hydrogen bonds do not persist.[10]

NMR techniques are frequently used to probe molecular dynamics and conformation. Slow exchange between two or more chemically distinct conformations can be directly investigated on the basis of chemical shift measurements, line-shape analysis, T_2 measurements, and saturation transfer experiments.[11-13] Under favorable conditions, relaxation parameters such as the spin–lattice relaxation time, T_1, and NOE enhancement can yield information on molecular reorientation times.[11,14] In addition, it has been shown that internal motions which occur on the time scale of molecular reorientation can significantly alter the form of the rotational spectral density functions. The various dependencies of the relaxation parameters on the spectral density functions can then be used to extract motional information, in the form of an order parameter, at unique nuclear sites.[15,16]

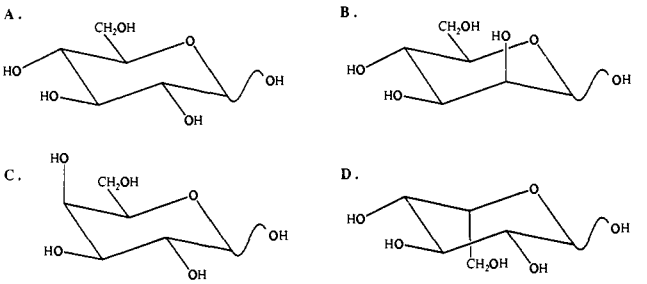

Figure 1. Standard $^4C_1$ chair conformation of (A) D-glucose, (B) D-mannose, (C) D-galactose, and (D) L-idose. Individual anomers are not shown.

Molecular mechanics and dynamics calculations have become widely used in the conformational and dynamical analysis of biomolecules.[17] Rotational barriers between low-energy conformers have been investigated with torsion-angle driving and related techniques,[18,19] and restrained and unrestrained dynamics simulations have complemented these studies.[20]

In this manuscript, experimental order parameters and molecular dynamics simulations are used to assess the picosecond dynamics of a variety of α- and β-anomers of hexopyranose monosaccharides (see Figure 1). It is found that all ring carbons in all sugars studied exhibit similar motional disorder on this time scale, indicating that the motions involved are independent of hydroxyl or hydroxymethyl group orientation. Dynamics

* Author to whom correspondence should be addressed.

® Abstract published in *Advance ACS Abstracts*, September 1, 1993.

(1) Ferro, D. R.; Provasoli, A.; Ragazzi, M. *Carbohydr. Res.* **1990**, *195*, 157–167.
(2) Casu, B.; Oreste, P.; Torri, G.; Zoppetti, G.; Choay, J.; Lormeau, J.-C.; Petitou, M.; Sinaÿ, P. *Biochem. J.* **1981**, *197*, 599–609.
(3) Ferro, D. R.; Provasoli, A.; Ragazzi, M.; Torri, G.; Casu, B.; Gatti, G.; Jaquinet, J.-C.; Sinaÿ, P.; Petitou, M.; Choay, J. *J. Am. Chem. Soc.* **1986**, *108*, 6773–6778.
(4) Ragazzi, M.; Ferro, D. R.; Perly, B.; Sinaÿ, P.; Petitou, M.; Choay, J. *Carbohydr. Res.* **1990**, *195*, 169–185.
(5) Ragazzi, M.; Ferro, D. R.; Provasoli, A. *J. Comput. Chem.* **1986**, *7*, 105–112.
(6) Forster, M. J.; Mulloy, B. *Biopolymers* **1993**, *33*, 575–588.
(7) Casu, B.; Petitou, M.; Provasoli, M.; Sinaÿ, P. *Trends Biochem. Sci.* **1988**, *13*, 221–225.
(8) Brown, G. M.; Levy, H. A. *Acta Crystallogr.* **1973**, *29*, 790.
(9) Bock, K.; Lemieux, R. U. *Carbohydr. Res.* **1982**, *100*, 63.
(10) Adams, B.; Lerner, L. *J. Am. Chem. Soc.* **1992**, *114*, 4827–4829.
(11) Ernst, R. R.; Bodenhausen, G.; Wokaun, A. *Principles of Nuclear Magnetic Resonance in One and Two Dimensions*; Oxford University Press: New York, 1988.
(12) Schlichter, C. P. *Principles of Magnetic Resonance*; Springer-Verlag: New York, 1980.
(13) Kaplan, J. I.; Fraenkel, G. *NMR of Chemically Exchanging Systems*; Academic Press: New York, 1980.
(14) Neuhaus, D.; Williamson, M. *The Nuclear Overhauser Effect in Structural and Conformational Analysis*; VCH Publishers, Inc.: New York, 1980.
(15) Lipari, G.; Szabo, A. *J. Am. Chem. Soc.* **1982**, *104*, 4546–4559.
(16) McCain, D. C.; Markley, J. L. *J. Am. Chem. Soc.* **1986**, *108*, 4259–4264.
(17) Brady, J. *Adv. Biophys. Chem.* **1990**, *1*, 155–202.
(18) Arteca, G. A. *J. Comput. Chem.* **1993**, *14*, 718–727.
(19) Kolossvary, I.; Guida, W. C. *J. Comp. Chem.* **1993**, *14*, 691–698.
(20) van Gunsteren, W. F.; Berendsen, H. J. *Angew. Chem., Int. Ed. Engl.* **1990**, *29*, 992–1023.

0002-7863/93/1515-9196$04.00/0

calculations indicate that this disorder could result from ring deformations in the form of ring librations.

We have also investigated the dynamics of the hydroxymethyl groups. In the monosaccharides studied, the hydroxymethyl groups do not undergo free rotation on the molecular reorientation time scale and have the same motional freedom as the hydroxymethyl groups in aqueous sucrose. This suggests that the hindered rotation observed on the picosecond time scale in sucrose may not be caused by hydrogen bonding between the pyranose and furanose rings, as previously suggested.

Experimental Section

All experiments were performed on Varian Unity 500- and 300-MHz NMR spectrometers at temperatures ranging from −10 to 30 °C. Data were processed off-line on Sun Sparcstations using standard Varian software. T_1 values were determined by the standard inversion recovery method (180–τ–90–acquisition) performed with randomized τ delays and ^{1}H decoupling throughout the entire experiment. Nuclear Overhauser enhancements were determined by acquiring two carbon spectra, one with decoupling throughout the entire experiment and one with decoupling only during acquisition. All experiments were performed with eight steady-state scans and a preacquisition delay equal to at least 5 times the longest T_1 in the sample, and typical signal-to-noise ratios were at least 100:1 in single-pulse experiments.

All samples were 1.0 M in 1:1 DMSO-d_6:D_2O. DMSO-d_6 was obtained from Isotech, Inc. (Miamisburg, OH). D_2O was obtained from Cambridge Isotope Laboratories (Woburn, MA). D-Galactose was obtained from Aldrich (Milwaukee, WI). D-Glucose, D-mannose, and L-idose were obtained from Sigma (St. Louis, MO). All monosaccharides were used as supplied without further purification.

Computer Simulations

Dynamics calculations were performed with the MM3* force field as implemented in Macromodel 3.5×,[21] running on an IBM RS-6000/320 workstation. This force field differs from the original MM3(90) in that it uses the partial charge treatment of electrostatics instead of the MM3 standard dipole–dipole electrostatics. All dynamics were performed at constant temperature with a 1-fs step size, and coupling between the bath and the molecule was updated every 0.2 ps. The temperature was initially ramped from 0 to 300 K over a 20-ps time period and allowed to equilibrate at 300 K for an additional 20 ps. Structures were then sampled over a subsequent MD run at 300 K. In order to assess the dependence of the calculations on various user-defined variables, the following parameters were altered (both individually and in combination) in a series of calculations: (1) simulation length (500, 1000, and 1500 ps), (2) sampling frequency (3, 5, and 10 structures/ps), (3) cut-off distance for nonbonded interactions (12 and 20 Å), (4) hydrogen-bonding potentials (MM3* defined potentials and a 6,12 Lennard-Jones potential), (5) solvation treatment (no solvent and GB/SA (generalized Born/solvent approximation) water solvation[22]), and (6) initial hydroxymethyl rotameric state. All initial conformations for the dynamics calculations were first minimized to a derivative convergence criterion of 0.01 kJ/Å.

Order parameters (*vide infra*) were derived directly from the angular trajectories of the C–H vectors. The order parameter was defined as the asymptotic value of the time correlation function given by[23,24]

$$C(\Delta t) = \frac{1}{5}\sum_{m=-2}^{2} \overline{\langle Y_{2m}[\Omega(t)]\, Y_{2m}^*[\Omega(t+\Delta t)]\rangle} \qquad (1)$$

where $Y_{2m}[\Omega(t)]$ are the spherical harmonics of order m, the brackets indicate integration over the angular variables $\Omega(t)$, and the overline indicates the time average. The spherical harmonics were calculated at discrete time intervals t and $t + \Delta t$ and integrated over the angular variables θ and ϕ to yield a correlation value $C(\Delta t)$ for each structure. This value was then averaged over all structures to derive the time average.

All structural parameters derived from the dynamics calculations (dihedral angles and order parameters) were determined using an in-house program.

Theory

The general theory of the effects of internal motion on the form of the spectral density function is given in great detail elsewhere,[15,25] and only a brief summary is given below. The present description assumes dipolar relaxation only and overall isotropic reorientation.

For a ^{13}C nucleus relaxed by neighboring ^{1}H nuclei, the spin–lattice relaxation time (T_1) and nuclear Overhauser enhancement factor (η) are given by[16]

$$\frac{1}{T_1} = \frac{1}{10}\left(\frac{h\gamma_H\gamma_C}{2\pi}\right)^2 \sum_H \frac{1}{\langle r_{CH}^{\,3}\rangle^2}[J(\omega_H - \omega_C) + 3J(\omega_C) + 6J(\omega_H + \omega_C)] \qquad (2)$$

$$\eta = \left(\frac{\gamma_H}{\gamma_C}\right)\frac{6J(\omega_H + \omega_C) - J(\omega_H - \omega_C)}{J(\omega_H - \omega_C) + 3J(\omega_C) + 6J(\omega_H + \omega_C)} \qquad (3)$$

where $J(\omega)$ is a spectral density function, ω_H and ω_C are the Larmor frequencies for the proton and carbon nuclei, and γ_H and γ_C are the gyromagnetic ratios. The r_{CH} terms are the C–H internuclear distances, which are summed over all protons in the molecule for each carbon site.

The spectral density, $J(\omega)$, is the Fourier transform of the autocorrelation function, which for a rigid sphere is an exponentially decaying function with time constant τ_c. The spectral density has the form

$$J(\omega) = \int_0^\infty \langle Y_{2m}[\Omega(0)]\, Y_{2m}^*[\Omega(t)]\rangle \cos(\omega t)\, dt \qquad (4)$$

where $Y_{2m}(\Omega)$ are the second order spherical harmonics. For a rigid, isotropically tumbling molecule, eq 4 has the solution

$$J(\omega) = \frac{\tau_c}{1 + \omega^2\tau_c^{\,2}} \qquad (5)$$

Internal motions can also contribute to the correlation function, and these motions are governed by a correlation time which is generally treated as statistically uncorrelated with the overall motion. This makes the autocorrelation function bimodal, and a single correlation time no longer accurately describes the system. Generally, internal motions alone do not allow the internuclear vector to sample all possible orientations, and the exponential decay function describing the internal motion contribution to the correlation function has an asymptotic value greater than zero. Very fast internal motions will reach this plateau quickly, with the subsequent decay being determined solely by the overall motion. Internal motions which occur on the same time scale as overall motion will complicate the decay over the entire time range. Very slow motions will have no significant effect on the form of the correlation function. The general form for the spectral density function in the presence of internal motion is[15]

$$J(\omega) = S^2\frac{\tau_c}{1 + \omega^2\tau_c^{\,2}} + (1 - S^2)\frac{\tau}{1 + \omega^2\tau^2} \qquad (6)$$

where S^2 is an order parameter which describes the extent of the internal motion (essentially the plateau value for the internal motion decay function) and τ is an effective correlation time which is composed of both the overall and internal correlation times ($\tau^{-1} = \tau_c^{-1} + \tau_{int}^{-1}$). This form for the spectral density

(21) Mohamadi, F.; Richards, N. G. J.; Guida, W. C.; Liskamp, R.; Caufield, C.; Chang, G.; Hendrickson, T.; Still, W. C. Macromodel V3.5X. *J. Comput. Chem.* **1990**, *11*, 440–467.

(22) Still, W. C.; Tempczyk, A.; Hawley, R. C.; Hendrickson, T. *J. Am. Chem. Soc.* **1990**, *112*, 6127–6129.

(23) Lipari, G.; Szabo, A.; Levy, R. M. *Nature* **1982**, *300*, 197–198.

(24) Levy, R. M.; Karplus, M.; McCammon, J. A. *J. Am. Chem. Soc.* **1981**, *103*, 994–996.

(25) Lipari, G.; Szabo, A. *J. Am. Chem. Soc.* **1982**, *104*, 4559–4570.

function is analogous to those derived to describe anisotropic motion.[26] As can be seen from this equation, a value for S^2 of 1.0 (rigid molecule) yields the normal spectral density as given in eq 5. Also, in the limit of very fast internal motions ($\tau \ll \tau_c$), eq 6 reduces to

$$J(\omega) = S^2 \frac{\tau_c}{1 + \omega^2 \tau_c^2} \qquad (7)$$

where the spectral density function is now simply scaled by the order parameter.

The order parameter, S^2, the overall correlation time, τ_c, and the effective correlation time, τ, can be obtained by simultaneously fitting eqs 2 and 3 using eq 6 with T_1 and NOE data at multiple field strengths. If the system is adequately described by eq 7, then only τ_c and S^2 need be determined, which can be done with T_1 and NOE data at any field strength. In theory, S^2, τ_c, and τ can be obtained at a single field strength by using T_1, T_2, and NOE measurements.[27,28] However, estimates of heteronuclear T_2 values are generally more sensitive to experimental artefacts (spin-echo pulse train, proton-decoupling scheme, etc.) than T_1 and NOE measurements. In addition, chemical exchange on time scales far removed from τ_c can affect the observed T_2 value and complicate the analysis of short-time dynamics. Therefore, to increase accuracy and provide additional relaxation parameters, T_1 and NOE data were acquired at two field strengths.

The data were fit using both eqs 6 and 7 with a least squares fitting routine. Errors in T_1 and NOE values were estimated to be 5 and 10%, respectively, which resulted in uncertainties in S^2 of 5–8% and in τ_c of 10–20%. The deviations between experimental and predicted T_1 and NOE values were well below the 5 and 10% error estimates over all temperatures and field strengths. Order parameters for the ring carbon sites were calculated both individually and as an average over the entire ring. Order parameters for the hydroxymethyl carbons were calculated individually and not included in the ring averages. NOE factors ranged from 0.4 to 1.9 over the experimental temperature range, but only η values in the range of 0.4 to 1.7 were used in the calculations to avoid points near the theoretical NOE maximum (1.988) where the NOE is insensitive to correlation time. C–H bond distances were taken directly from previous work on sucrose.[16,29] These distances should not be significantly different for the monosaccharides. The total $\sum_i \langle r_{CH}^3 \rangle^{-2}$ values for the ring and hydroxymethyl carbons were 5.30×10^5 and 1.11×10^6 nm^{-6}, respectively. The values used for $(\hbar \gamma_H \gamma_C)^2/10$ and (γ_H/γ_C) were 3.602×10^3 nm^6 s^{-2} and 3.977, respectively.

Results

NMR. ^{13}C resonance assignments for the sugars were taken from previous work.[30,31] In solution, both the α and β isomers for all of the pyranose sugars were present. In addition, the α and β furanose isomers are also present in L-idose and D-galactose. Experimental order parameters were determined for the following isomeric forms of the sugars (p = pyranose; f = furanose; ratios determined from relative intensities of the observed resonances): α-D-glucopyranose (αp:βp ~ 80:20), α- and β-D-galactopyranose (αp:βp:αf:βf ~ 30:60:5:5), α-D-mannopyranose (αp:βp ~ 80:20), and α- and β-L-idopyranose (αp:βp:αf:βf ~ 35:45:10:10). Interconversion between the various isomers was ignored in the analysis since these rates have been determined to be on the order of tens of seconds[30] and the longest T_1 values were approximately 0.7 s.

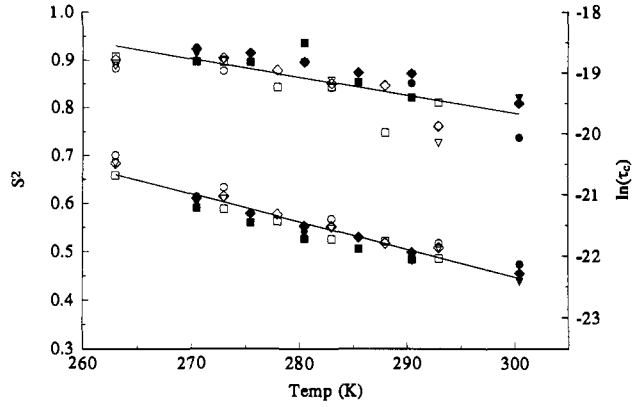

Figure 2. Experimental order parameters, S^2 (upper trace, left y-axis), and correlation times, τ_c (lower trace, right y-axis), for the ring carbons in α-D-glucose (circles), α/β-D-galactose (triangles), α-D-mannose (diamonds), and α/β-L-idose (squares). Values shown are least squares fits to all ring carbons simultaneously. Closed and open symbols are for data at ^{13}C 125 and 75 MHz, respectively. Best fit lines are also shown: $S^2 = -0.0038T + 1.9331$ and $\tau_c = 1.56 \times 10^{-4} \exp(-0.0453T)$.

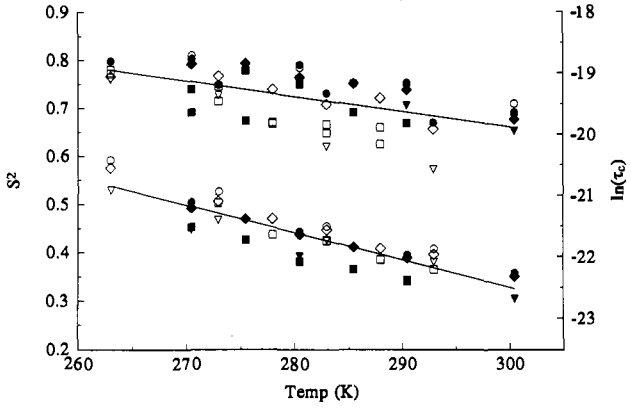

Figure 3. Experimental order parameters, S^2 (upper trace, left y-axis), and correlation times, τ_c (lower trace, right y-axis), for the hydroxymethyl carbons in α-D-glucose (circles), α/β-D-galactose (triangles), α-D-mannose (diamonds), and α/β-L-idose (squares). Closed and open symbols are for data at ^{13}C 125 and 75 MHz, respectively. Best fit lines are also shown: $S^2 = -0.0032T + 1.6273$ and $\tau_c = 1.11 \times 10^{-4} \exp(-0.0446T)$.

Figures 2 and 3 show the experimental order parameters and correlation times (using eq 7) for the ring and hydroxymethyl carbons, respectively. These results indicate that both the ring and hydroxymethyl carbons have a significant amount of motional disorder. Experimental order parameters for the ring carbons averaged from 0.91 to 0.78 over the range of temperatures studied. The order parameters for the hydroxymethyl carbons averaged from 0.80 to 0.66, indicating significantly more motional freedom than the ring carbons. The data at 125 and 75 MHz are nearly identical, as are the data for all sugars studied. Attempting to fit the data using eq 6 results in similar values for S^2 and τ_c and vanishingly small values for the effective correlation time, τ, verifying the use of eq 7 in the limit $\tau \ll \tau_c$. Order parameters were also identical within experimental error for all carbon sites in the sugar ring. Both the ring and hydroxymethyl carbons exhibited a similar temperature dependence (see Figures 2 and 3).

Several models can be used to extract molecular information from experimental order parameters. The first assumes that the C–H vector diffuses in a cone of semiangle θ_0.[25,28] In this motional model, the order parameter is given by

$$S^2 = \left[\frac{\cos\theta_0(1 + \cos\theta_0)}{2}\right]^2 \qquad (8)$$

Another model is to assume that the motion involved can be

(26) Woessner, D. E. *J. Chem. Phys.* **1962**, *36*, 1–4.
(27) Barbato, G.; Ikura, M.; Kay, L. E.; Pastor, R. W.; Bax, A. *Biochemistry* **1992**, *31*, 5269–5278.
(28) Nicholson, L. K.; Kay, L. E.; Baldisseri, D. M.; Arango, J.; Young, P. E.; Bax, A.; Torchia, D. A. *Biochemistry* **1992**, *31*, 5253–5263.
(29) McCain, D. C.; Markley, J. L. *J. Magn. Reson.* **1987**, *73*, 244–251.
(30) Snyder, J. R.; Serianni, A. S. *J. Org. Chem.* **1986**, *51*, 2694–2702.
(31) King-Morris, M. J.; Serianni, A. S. *J. Am. Chem. Soc.* **1987**, *109*, 3501–3508.

Table I. Experimental and Theoretical Order Parameters

	simulation			experiment[d]		
carbon	S^2 [a]	θ_0 [b]	γ_0 [c]	S^2	θ_0	γ_0
C1	0.967	9	11	0.89–0.80	16–22	21–29
C2	0.962	9	12	0.90–0.79	15–23	20–30
C3	0.965	9	12	0.89–0.75	16–25	21–33
C4	0.967	9	11	0.91–0.76	14–24	19–32
C5	0.971	8	10	0.93–0.79	13–23	16–30
ring average	0.966	9	11	0.91–0.78	14–23	19–31
C6	0.909	14	19	0.80–0.66	22–30	29–40

[a] Values obtained from dynamical simulations on α-D-glucose as described in the text. [b] Angle, in degrees, derived from eq 8. [c] Angle, in degrees, derived from eq 9. [d] Average values from all monosaccharides over the experimental temperature range.

described by torsional libration about the midpoint of a square-well potential with torsional limits of $\pm\gamma_0$.[29,32] For tetrahedral bond angles, the order parameter is given by

$$S^2 = \left(\frac{1}{27}\right)\left(3 + 8\frac{\sin^2\gamma_0}{\gamma_0} + 16\frac{\sin^2 2\gamma_0}{2\gamma_0}\right) \qquad (9)$$

The values obtained using these models with the theoretical and experimental order parameters are given in Table I.

Molecular Dynamics. The molecular trajectories were insensitive to changes in the parameters described in the Experimental Section. The only significant change observed with any of the varied parameters was a change in the relative energies of the different rotameric states of the hydroxymethyl group with the different hydrogen-bonding potentials. The *trans-gauche*, *gauche-trans*, and *gauche-gauche* rotamers will be referred to as *t-g*, *g-t*, and *g-g*, respectively, with the O5–C5–C6–O6 torsion angle stated first and the C4–C5–C6–O6 angle second. With the MM3* defined hydrogen bond potentials, all three rotamers in α-D-glucose are predicted to be energetically equivalent (ΔE of 0.0, 0.8, and 1.6 kJ/mol for the *g-t*, *t-g*, and *g-g* conformers, respectively). This conflicts with the absence of the *t-g* conformer in glucopyranoses.[33] The relative stability of the *t-g* conformer observed in the calculations with MM3* is due to the presence (and overemphasis) of a hydrogen bond between O4-H and O6, as previously observed with other potential functions.[34] The use of a 6,12 Lennard-Jones hydrogen bond potential (ΔE of 0.0, 1.4, and 10.1 kJ/mol for the *g-t*, *g-g*, and *t-g* conformers, respectively) gave results consistent with the experimental data. Using these parameters, the chair stabilization energies, $\Delta E(^4C_1 - {}^1C_4)$, for α-D-glucose and α-L-idose were calculated to be −18.2 and 4.1 kJ/mol, respectively. The results are in excellent agreement with previous force field and structural studies on ido- and glucopyranoses,[5,34,35-37] as can be seen in Table II for α-D-glucose. In addition, the angular distributions about the minimum for all of the above calculations were essentially identical. The calculations are therefore a robust investigation of the picosecond dynamics of the monosaccharides. All results from dynamics calculations reported in this manuscript (order parameters, dihedral angles, etc.) were taken from 5000 structures sampled over a 1000-ps MD simulation on α-D-glucose using MM3* with a 6,12 Lennard-Jones hydrogen bond potential and GB/SA water solvation.

Figure 4 shows the angular distributions for the ring and hydroxymethyl carbons in α-D-glucose. It is clear that both types of carbon sites can sample a range of orientations, with the hydroxymethyl group exhibiting significantly more motional freedom. In simulations on α-D-glucose initially in the *t-g* or *g-g* conformation, the hydroxymethyl group rapidly (<50 ps) converted to the *g-t* conformer and remained in that conformation with no further transitions after equilibration. In simulations on either α-D-glucose or α-L-idose initially in the $^4C_1$ or $^1C_4$ ring conformation, no transitions between the chair forms were observed, with each form exhibiting similar motions. The theoretical order parameters derived from the dynamics simulations and the angles derived from eqs 8 and 9 are given in Table I. The experimental and theoretical values agree well, but the experimental values are consistently lower than those predicted by the simulations. This may reflect an undersampling of the full range of conformational space available to the various carbon sites in the simulations.

To quantify the degree of flexibility observed in the simulations, a moments analysis of the angular distributions was performed and the results are given in Table II. The *n*th moment of a distribution described by some function $f(x)$ is given by[38]

$$\mu_n = \sum_i (x_i - \bar{x})^n f(x_i) \qquad (10)$$

where $\bar{x}$ is the mean value. The first moment is zero by definition and is therefore not considered. The second moment is the variance (square of the standard deviation) and describes the broadness of the distribution. The third moment describes the skewness of the distribution (zero for a perfectly symmetrical distribution), and the fourth moment describes the "peakedness" of the distribution. The fourth moment, referred to as kurtosis,[38] describes the molecule's tendency to deviate from the average conformation and can be viewed as a measure of torsional flexibility. Although a distribution is completely described by all of its moments, the first four are usually sufficient to extract most meaningful information. Higher order moments were therefore not considered in this analysis. It is clear from Table II that the hydroxymethyl group exhibits considerably more motion than the ring carbons, as expected. The angular standard deviation for the hydroxymethyl group is nearly twice that for the ring carbons, and the third and fourth moments are larger by more than an order of magnitude.

In addition to a moments analysis, the free energy surface around the energetic minimum was investigated by applying a Boltzmann distribution function to the molecular trajectories. The chosen distribution function was of the form

$$\chi_i = \exp\left(\frac{-\Delta G_i^*}{RT}\right) \qquad (11)$$

where χ_i is the fractional population of the *i*th conformer, ΔG_i^* is the free energy difference between the *i*th conformer and the global minimum, R is the gas constant, and T is the temperature. This analysis is similar to activated-complex theory where the transition-state complex is assumed to be in thermal equilibrium with the products and reactants.[39] The system can then be treated formally with statistical thermodynamics. The assumption in this treatment is that the population distribution of the various conformers (represented by discrete dihedral angles) is in thermal equilibrium. Equation 11 can be rearranged to obtain free energy values for each conformer

$$\Delta G_i^* = -RT\ln(\chi_i) \qquad (12)$$

This type of analysis has also been used to investigate the picosecond dynamics of tyrosine side chains in bovine pancreatic trypsin inhibitor.[40] In our calculations, only torsion angles within two standard deviations of the mean were used, and the resulting

(32) London, R. E.; Avitabile, J. *J. Am. Chem. Soc.* **1978**, *100*, 7159–7165.
(33) Marchessault, R. H.; Perez, S. *Biopolymers* **1979**, *18*, 2369–2374.
(34) Ha, S. N.; Giammona, A.; Field, M.; Brady, J. W. *Carbohydr. Res.* **1988**, *180*, 207–221.
(35) Giuliano, R. M.; Bryan, R. E.; Hartley, P.; Peckler, S.; Woode, M. K. *Carbohydr. Res.* **1989**, *191*, 1–11.
(36) Brady, J. W. *J. Am. Chem. Soc.* **1986**, *108*, 8153–8160.
(37) Brown, G. M.; Levy, H. A. *Acta Crystallogr., Sect. B* **1979**, *35*, 656–659.
(38) Lipkowitz, K. B.; Peterson, M. A. *J. Comput. Chem.* **1993**, *14*, 121–125.
(39) Moore, W. J. *Physical Chemistry*; Prentice-Hall, Inc.: Englewood Cliffs, NJ, 1972.
(40) McCammon, J. A.; Wolynes, P. G.; Karplus, M. *Biochemistry* **1979**, *18*, 927–942.

Table II. Results of Moments Analyses of Angle Distributions in α-D-Glucose

torsion angle	experimental value[a]	average angle[b]	standard deviation	second moment	third moment	fourth moment
C1–C2–C3–C4	−51.3	−53.9	2.5	6.0	9.3	379.4
C2–C3–C4–C5	53.3	53.1	2.6	6.6	−13.9	451.2
C3–C4–C5–O5	−57.5	−57.0	2.7	7.3	25.5	549.3
C4–C5–O5–C1	62.2	60.5	2.6	6.5	−18.4	466.9
C5–O5–C1–C2	−60.9	−60.3	2.4	5.7	1.2	299.4
O5–C1–C2–C3	54.1	54.9	2.6	6.7	−1.6	403.9
ring average			2.5	6.5	11.7[c]	425.0
O5–C5–C6–O6	70.2	68.4	4.6	21.0	152.7	5415.2

[a] Experimental values taken directly from ref 37. [b] Values determined from dynamics calculations on α-D-glucose as described in the text. [c] Absolute values used to calculate ring average.

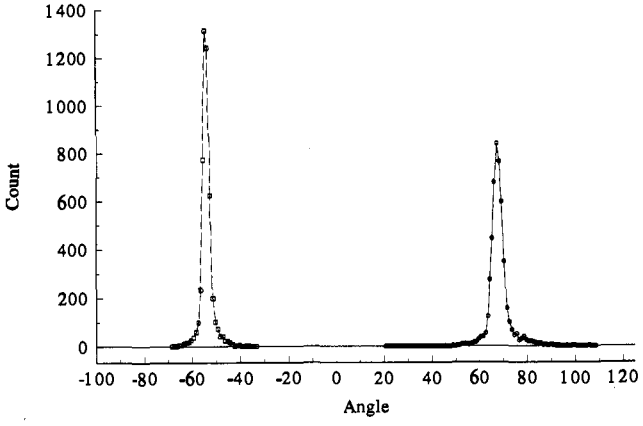

Figure 4. Angular distribution trajectories from molecular dynamics simulations on α-D-glucose as described in the text. Data are shown for the C1–C2–C3–C4 (left, open squares) and O5–C5–C6–O6 (right, open circles) torsion angles.

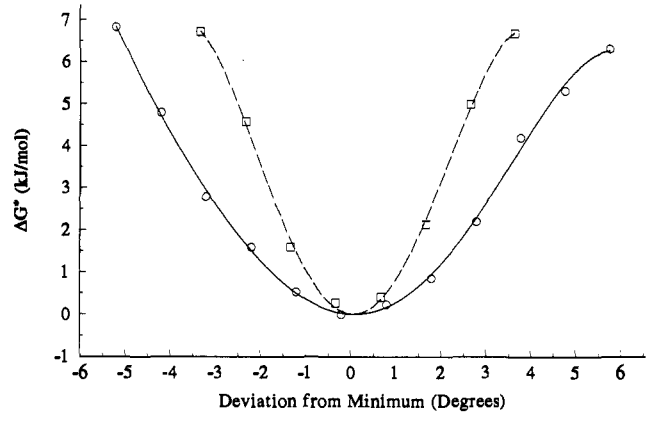

Figure 5. Free energy surfaces for the ring carbons (open squares) and hydroxymethyl carbons (open circles) derived from the angular distributions as described in the text. Also shown are the best fit fifth-order polynomials for aid in visualization.

free energy surfaces are shown in Figure 5. It must be emphasized that the energy surfaces derived in this procedure result only from those conformations which were sampled during the length of the dynamics simulation, with the assumption that the allowed conformational space is sampled to a statistically significant level. Undersampling or insufficient simulation length may skew the conformer populations and result in misleading or erroneous values for ΔG. In addition, energy minima which were not sampled in the trajectory (i.e. different rotameric states for the hydroxymethyl group) will not affect the shape of the energy surface. Significantly longer calculations ($\gg$1 ns) or increases in temperature may simulate these transitions and allow for statistical sampling.

Figure 6 shows an example of the ring deformations observed in α-D-glucose. For clarity, only the heavy atoms are shown, but it is apparent that the C–H vectors can sample a significant amount

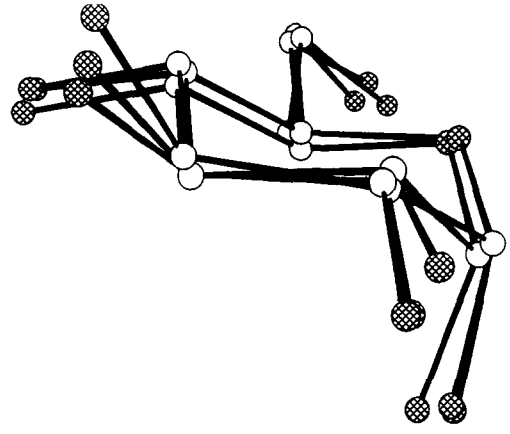

Figure 6. Ring deformations observed in α-D-glucose during dynamical simulation as described in the text. Structures shown correspond to C1–C2–C3–C4 torsion angles of −35.8°, −53.9° (equilibrium structure) and −66.7°. Only heavy atoms are shown (open circles correspond to oxygen atoms).

of conformational space even in the absence of overall molecular reorientation.

Discussion

The similarity among the various monosaccharides is remarkable, as is the indistinguishability of the ring carbon sites. These results indicate that hydroxyl and hydroxymethyl group orientations have little impact on the picosecond dynamics of simple sugars. In addition, the large values for the order parameters indicate that all carbon sites maintain a single global conformation (ring conformation or hydroxymethyl rotamer).

The ring carbon results are most significant in the case of L-idose. Idose and its derivatives have been shown, using coupling constant analyses, to adopt several different ring conformations, and this flexibility has been implicated in the biological function of idose-containing oligosaccharides.[1,7] Our results help define a rough window for the conformational interconversion correlation time. Since the spectral density functions will only be significantly affected by internal motions which occur as fast or faster than overall motion, any chair–chair interconversion must be occurring on a time scale much longer than τ_c. The correlation times of our samples range from 0.2 to 1.3 ns, and an estimate for the minimum correlation time for ring conformational changes would be >1 ns. Since only single, sharp ^{13}C resonances were observed at all temperatures for idose, the exchange must be occurring fast on the chemical shift time scale. As an example, a chemical shift difference between two conformers of 1 ppm would require an interconversion rate greater than 125 Hz to average the resonances to a single line. A ^{13}C chemical shift difference of 1 ppm is not unreasonable for different ring conformations, and this difference would place an upper limit on the interconversion time of roughly 1 ms. Given both of these observations, an estimated window for chair–chair (or chair–boat) interconversion in idose is 10^{-9} to 10^{-3} s. Motions in this time regime may be amenable to analysis with $T_{1\rho}$ experiments, and this investigation is currently underway.

Crystal structures and coupling constant analyses of the hydroxymethyl groups of a wide range of sugars have shown that, in general, the *g-g*, *g-t*, and *t-g* (galactose only) rotamers all have significant populations at ambient temperatures.[33] The magnitude of the order parameter as well as the dynamics results suggests that exchange between these conformations does not occur on the picosecond time scale. Again, since only a single ^{13}C resonance is observed for the hydroxymethyl group, an approximate time scale for hydroxymethyl rotation is 10^{-9} to 10^{-3} s. Our results for the hydroxymethyl groups are virtually identical to the results obtained for aqueous sucrose.[29] The cause of the hindered rotation in these groups in sucrose has been attributed to hydrogen bonding and steric effects based on hard-sphere calculations and neutron diffraction studies.[8,9] While the order parameter results on sucrose correlated roughly with these studies (except for fructose C6, which was predicted to have relatively free internal rotation in aqueous solution), our results suggest that the large order parameters observed for all hydroxymethyl groups in sucrose do not necessarily arise from unique interactions, such as hydrogen bonding between the glucose and fructose residues, which are not available to the monosaccharides. All hydroxymethyl groups of the monosaccharides in this study exhibited a lack of rotation.

The ring carbons in the simple sugars showed a temperature dependence similar to that of the hydroxymethyl carbons (see Figures 2 and 3). This result is contrary to the case of sucrose, where the hydroxymethyl groups did exhibit a temperature dependence (similar to the monosaccharides) but the ring carbons did not. This seems to indicate that large substituents (such as a furanose ring) tend to mediate the amplitude of the ring deformations and dampen the temperature dependence. In addition, individual carbon sites in the ring are nearly identical in the monosaccharides, whereas C1$^{\beta}$ (pyranose ring) in sucrose is a bridgehead carbon and is highly ordered relative to the other carbon sites (S^2 = 0.962 for C1$^{\beta}$ *vs* 0.861–0.898 for the other sites).[16]

The moments of the angular trajectories derived from the dynamics calculations correlate well with the experimental order parameters, with the hydroxymethyl groups exhibiting much more motion than the ring carbons while still remaining in a single rotameric state (see Table II). The ring deformations shown in Figure 6 are reasonable deviations from an ideal $^4C_1$ chair conformation which can average the C_{ring}–H internuclear vector over a significant amount of conformational space. Although the theoretical order parameters are somewhat higher than the experimental values (see Table I), the relative agreement is good. The discrepancy may be due to undersampling of the configurational space, especially toward the extremes of the distribution, or to the force fields not completely describing the allowed range of motion. In any event, the qualitative agreement between theory and experiment is evidence that the motions observed in the simulations are a sufficient model for the picosecond dynamics of simple sugars.

The dynamics trajectories also allow for a qualitative comparison of the energy surfaces for the ring and hydroxymethyl carbons in the absence of fixed or restrained molecular geometries. Traditional approaches to the investigation of potential energy surfaces involve the driving of a molecular parameter (torsion angle, etc.) with subsequent energy calculations. While this technique is fast, it suffers from several problems, not the least of which is the generation of unrealistic molecular geometries which are far from the true reaction coordinate.[41] Dynamics calculations performed at an appropriately small step size are continually sampling the potential energy surface and are therefore better representations of the true reaction coordinate. The moments analyses of the angular distributions described in this manuscript and elsewhere[38] offer quantitative insight into the shape of the energy surface around the minimum. The second and fourth moments for glucose indicate that the energy surface for the hydroxymethyl group is broader and shallower than that for the ring carbons. The Boltzmann-type analysis of the angular trajectories (described by eq 12) enables one to construct a free energy surface, and a postulated form for this surface near the global minimum is shown in Figure 5. It should be mentioned that the free energy (ΔG^*) was used instead of the potential energy (ΔE) because the angular distributions should reflect entropic as well as enthalpic contributions. While this graph should be viewed qualitatively, the essential characteristics are derived directly from the dynamics calculations with no molecular constraints.

The dynamics results offer a motional model for the order parameters observed in the sugars. Unfortunately, there are very few experimental techniques which directly probe the time regime of dynamics calculations, which are generally on the order of nanoseconds or less. Therefore, detailed motional models cannot be obtained. Most NMR-derived constraints used to determine multiple conformations, such as NOEs or coupling constants, will be averaged if the conformer lifetimes are on the order of microseconds or shorter. The dynamics calculations sample only a small portion of this time regime and therefore cannot simulate motions which may average these parameters but occur on time scales longer than the simulation length. The advantage of experimental order parameters is that they are sensitive to motions which occur on time scales readily accessible to dynamics calculations and a direct comparison is possible.

Conclusions

In summary, our results show that, on the picosecond time scale, all C–H vectors in these four monosaccharides sample a significant amount of configurational space while maintaining a single global conformation. No evidence for ring interconversions or frequent hydroxymethyl rotation was observed. This result, combined with the observation of a single ^{13}C resonance for each carbon site, allows for the estimation of a hydroxymethyl rotation and idose chair–chair (or chair–boat) interconversion time scale of nano- to microseconds. The hydroxymethyl results are identical to those observed for aqueous sucrose, indicating that the hindered rotation observed for the hydroxymethyl groups in sucrose is not necessarily caused by hydrogen bonds between the pyranose and furanose moieties or any other interaction which is not available to the monosaccharides. The dynamical simulations also indicate that hydroxymethyl rotation is hindered, and the observed deformations in the $^4C_1$ chair are proposed as a motional model to account for the disorder at the ring carbon sites.

Acknowledgment. P.J.H gratefully acknowledges support from the University of Wisconsin Biotechnology Program. D.A.H. gratefully acknowledges support from the National Science Foundation and the Wisconsin Alumni Research Foundation. The authors thank Dr. Bruce Adams for stimulating conversations. This work was supported by the NIH (Grant R29 AR39801). The NMR spectrometer used was purchased in part with funds from the NSF (Grant CHE-8813550) and NIH (Grant SIO RRO 4981) shared instrumentation programs. The computers used for molecular dynamics calculations were purchased in part with funds from the NSF (Grant CHE-9007850).

(41) Burkert, U.; Allinger, N. L. *J. Comput. Chem.* **1982**, *3*, 40–46.